Microwave Induced Interfacial Nanobubbles

Lei Wang,[†] Xiaojun Miao,[†] and Gang Pan[*,†,‡]

[†]Research Center for Eco-Environmental Sciences, Chinese Academy of Sciences, Beijing 100085, China

[‡]School of Animal, Rural and Environmental Sciences, Nottingham Trent University, Brackenhurst Campus, Southwell NG25 0QF, United Kingdom

[*]Corresponding author: gpan@rcees.ac.cn

ABSTRACT

A new method for generating nanobubbles via microwave irradiation was verified and quantified. AFM measurement showed that nanobubbles with diameters ranging in 200 - 600 nm were generated at water-HOPG surface by applying microwave to aqueous solutions with 9.0 - 30.0 mg/L of dissolved oxygen. Graphite displays strong microwave absorption and transmits high thermal energy to surface. Due to high dielectric constant (20 °C, 80 F/m) and dielectric loss factor, water molecule has strong absorption ability for microwave. The thermal and non-thermal effects of microwave both had contributions to decrease gas solubility and that facilitated nanobubble nucleation. The yield of nanobubbles increased about ten times when irradiation time increased from 60 s to 120 s at 200 W microwave. The nanobubbles density increased from 0.8 to 15 numbers/μm^2 by improving working power from 200 to 600 W. An apparent improvement of nanobubbles yield was obtained between 300 and 400 W, and the resulting temperature was 34 - 52 °C. When the initial dissolved oxygen increased from 11.3 to 30.0 mg/L, the density of nanobubbles increased from 1.2 to 13 numbers/μm^2. The generation of nanobubbles could be well controlled by adjusting gas concentration, microwave power or irradiation time. The method maybe valuable in preparing surface nanobubbles quickly and conveniently for various applications, such as catalysis, hypoxia/anoxia remediation or as templates

to prepare nanoscale materials.

1. INTRODUCTION

Surface nanobubbles are gaseous domains that are typically tens to hundreds of nanometers in radius and 10 - 100 nm high. Nanobubbles were first reported by Parker et al.[1] for explaining the effect of hydrophobic long-range force. In 2000, two research groups reported the first images of nanobubbles on various hydrophobic surfaces in water by AFM which demonstrated the existence of nanobubbles directly[2, 3] and this is a significant milestone of nanobubbles study. Since then, nanobubbles have attracted increasing attention in various fields including nanofluidics,[4] nanomedicine,[5, 6] nanochemistry[7, 8] and environmental remediation.[9, 10, 11, 12] Investigations focus on unraveling the mystery behind nanobubble nucleation,[13, 14, 15, 16, 17], nanobubble stability mechanism including contamination layer and contact line pinning,[18, 19] quantifying bubble dynamics as a function of different parameters,[20, 21, 22, 23, 24] as well as developing potential applications in lubrication,[25] cleaning,[26, 27, 28] flotation of minerals[29] and synthesizing highly porous metallic surfaces.[30] To fully exploit these possibilities, there is the need to prepare various types of gas nanobubbles by simple methods, which can be used to generate nanobubbles in a controlled way.

Research advances on various physical aspects of surface nanobubbles in the past decade include methods of nanobubble generation based on solvent exchange,[20, 31, 32, 33] temperature gradient,[21, 34] plasmonic effect[35] and water electrolysis.[36, 37, 38, 39, 40] Alcohol–water exchange is proved to be an effective method that can generate large amount of air nanobubbles with high repeatability.[16, 41, 42] Its efficiency may be attributed to the transient and local gas supersaturation close to the surface, when the alcohol, having a high gas solubility, is replaced by water, having a lower gas solubility. This local supersaturation presumably triggers the nucleation of small gaseous domains, the nanobubbles. However, exchange of organic solvents with water has some limitations. It needs large amount of organic solvents and fast exchanging process and a stable surface resistant to organic solvents, meanwhile organic solvents are more likely to introduce contaminations to the system and make the analysis complicated. Methods without solvent exchange to nucleate nanobubbles are required for nanobubble researches. Generation of plasmonic nanobubbles has drawn attention in the past few years.[43, 44] Irradiation gold nanoparticles (AuNPs) with nanosecond laser pulses, at a wavelength that matches their plasmon resonance, is an approach commonly used to generate vapor nanobubbles in both water and biological mediums. This method only applies to certain plasmonic nanoparticles and presents a promising diagnostic and therapeutic avenue for various pathologies.[45, 46] In recent years, electrochemical method has been employed to produce nanobubbles on the surface of electrode. Zhang et al.[36] and Chen et al.[47] confirmed that electrolysis of water induced the formation of hydrogen nanobubbles on highly orientated pyrolytic graphite (HOPG) surfaces or Pt electrode. Oxygen nanobubbles were determined simultaneously as a by-product of obtaining hydrogen gas by water electrolysis.[48] However, the yield of oxygen nanobubble was much lower than that of hydrogen nanobubble.[37] More recently, Chen et al.[49] reported the generation of N_2 nanobubbles at Pt nanoelectrode by irreversible electrooxidation of hydrazine. However, nanobubble generation by electrolysis is restricted by the type of electrolyte. For now, only water with or without acid and hydrazine have been used as electrolyte. System temperature proved to be an important factor for the formation of nanobubbles, however, there is the need to advance this method with high efficient and low energy cost.

Microwave has pronounced thermal effect. The working principle of microwave is based on water molecule's fast shear flow and molecules friction.[50] Water molecules can rotate in time with electric field frequencies of 2.45 GHz in liquids. Due to this process, "internal friction" takes place in the polar medium, which leads to a direct heating of the mixture. Graphite presents strong microwave absorption ability because of its low resistance, being able to transmit high thermal energy to surface and resulting in dramatic temperature increase on surface.[51, 52, 53] The hot substrate may provide possibilities for interfacial nanobubbles formation in the aqueous solution. Microwave also presents non-thermal effect.[54] So far, there are no previous studies on the use of microwave for nanobubble generation.

Here, we propose to use microwave irradiation to generate interfacial nanobubbles. Oxygen was used as the gas source and nanobubbles were measured by AFM on HOPG surface. Influence factors to the formation process such as dissolved oxygen concentration, microwave power and irradiation time were studied. The objective of the study is to develop a convenient and efficient method for the controlled formation of nanobubbles.

2. EXPERIMENTAL

2.1. Chemicals and materials

Highly ordered pyrolytic graphite (HOPG) (1.2 cm × 1.2 cm, Bruker) was used as the substrate. HOPG was freshly cleaved before each experiment by peeling off the outermost layers with scotch tape.

Water with conductivity of 18.2 MΩ cm and pH 7.0 was obtained from a milli-Q system (Millipore Corp., Boston, MA). All glass containers for the liquid and tweezer were cleaned by acetone and ethanol, respectively, and then rinsed with water. The high pure oxygen (99.995%) was used as gas source to prepare nanobubbles. Experiments were carried out under ambient lab conditions.

2.2. Formation of nanobubbles by microwave

Microwave was used to prepare interfacial nanobubbles. The water was first degassed by keeping it for 1 h under a reduced pressure of 30 mbar. Then pure oxygen was aerated to the degassed ultrapure water with a flow rate of 160 mL per minute. A dissolved oxygen meter (JPSJ605, Shanghai REX Instrument Factory) was used to detect the concentration of dissolved oxygen (DO). In order to get the in situ nanobubbles images, the freshly cleaved HOPG was fixed on an iron stub by tape and put into the obtained 50 mL solution and then started the microwave treatment (OTG Motor Co. Ltd). The schematic diagram of nanobubbles generation was shown in figure 1. After this process, the HOPG covered with the microwave treated water was carefully and quickly transferred to the liquid cells and measured by AFM.

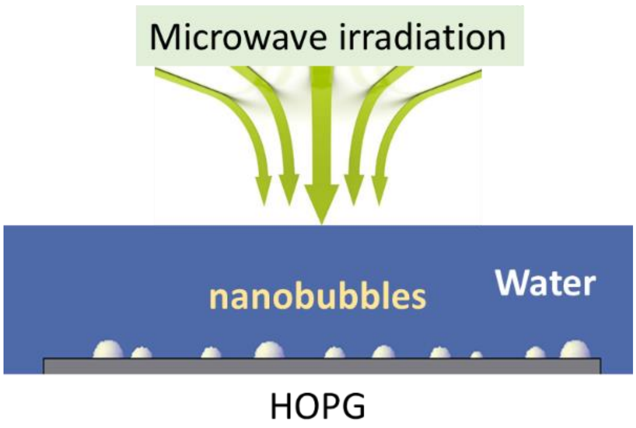

Figure 1. The schematic diagram of nanobubbles generation by microwave

2.3. Characterization of nanobubbles

The AFM used in the experiment was a Multimode Nanoscope IIIa from Digital Instruments (Bruker AXS GmbH), equipped with a liquid cell and an O–ring which sealed the cell and the substrate to prevent liquid leakage during the measurement. During the scanning, a vertical engage J scanner (120 × 120 μm^2) and silicon nitride cantilevers with their spring constant around 0.32 N/m were used. The probes were cleaned by immersing them in acetone and ethanol, respectively, and then rinsed with water. For imaging in fluid, the resonance frequency in tapping mode was from 7 kHz to 12 kHz and the amplitude set point was 80–90% of the free amplitude.

3. RESULTS

3.1. Generation of interfacial nanobubbles

The AFM image of HOPG substrate (Figure 2a) showed that no nanobubbles were observed when the freshly cleaved HOPG substrate was simply immersed into water with 9.0 mg/L of dissolved oxygen at ambient environment. Nanobubbles were formed after 30 s treatment by 400 W microwave irradiation (Figure 2b). The apparent diameter (lateral size) of nanobubbles was 200 - 600 nm. As shown in Figure 2c, oxygen nanobubbles still existed on the HOPG surface after 12 h. Once nanobubbles formed on the hydrophobic surface, they remained stable even in high temperature conditions and did not evolve into macroscopic bubbles.[55] The mechanism behind such stability may be related to the strong pinning at the three-phase boundary, which needs to be confirmed by more quantitative experiments. In the degassed control system, the treatment of microwave did not result in particle objects on the HOPG surface (Figure S1). A clear surface was revealed when the nanobubbles area was scanned under contact mode (Figure 2d). The tip always contacted with the substrate, and its force was strong enough to penetrate through soft nanobubbles. This result confirmed that microwave irradiation induced the formation of nanobubbles on the HOPG surface in water.

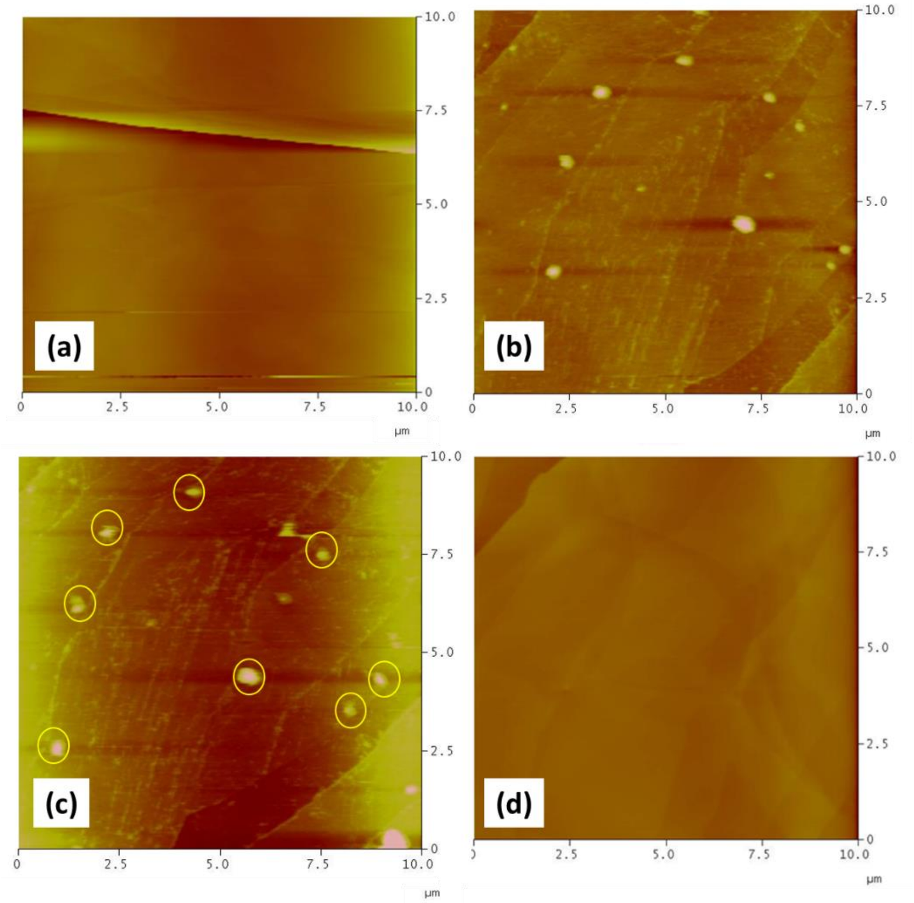

Figure 2. AFM images of HOPG substrate and nanobubbles: (a) the HOPG surface in water without microwave treatment, (b) images of nanobubbles generated by microwave irradiation, (c) nanobubbles images after 12 h scanning and (d) AFM contact mode of the same treatment sample. The scan sizes is 10 μm × 10 μm and height scale is 30 nm.

3.2. Effect of irradiation time and microwave working power

Typical images of nanobubbles generated by microwave as function of irradiation time were presented in Figure 3a-c. The irradiation power was set at 200 W and the initial oxygen concentration was 15.0 mg/L. The density of nanobubbles on HOPG increased significantly with the increase of irradiation time. AFM images in contact mode proved that the generated bubbles-like domains were indeed nanobubbles. The yield of oxygen nanobubbles increased about ten times when irradiation time increased from 60 s to 120 s (Figure 4).

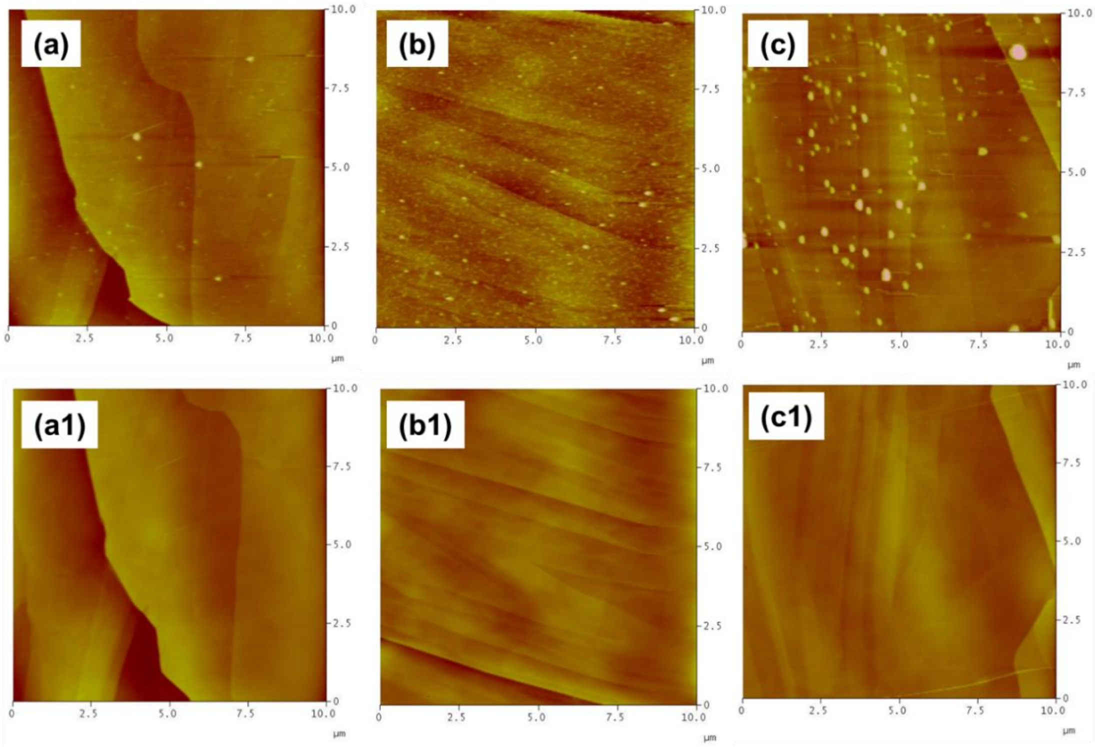

Figure 3. (a-c) AFM tapping mode height images of nanobubbles on water-HOPG surface with different microwave irradiation time: (a) 60 s, (b) 90 s and (c) 120 s; (a1-c1) AFM images of these same samples by contact mode. The scan sizes is 10 μm × 10 μm, height scale is 30 nm.

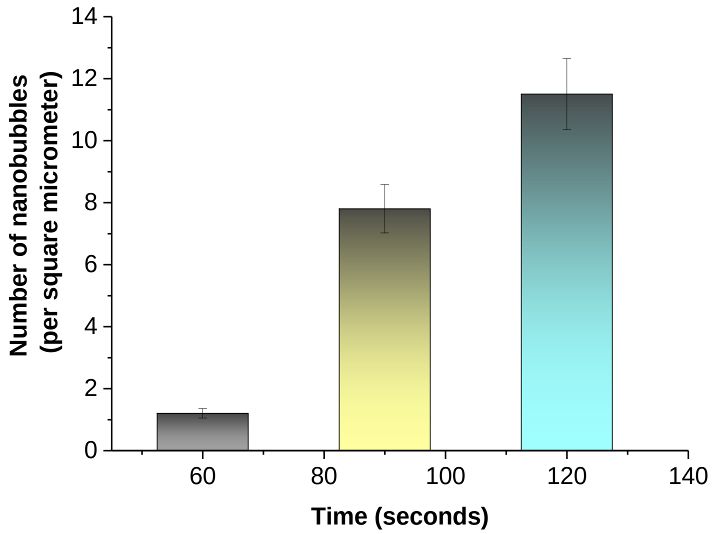

Figure 4. Effect of microwave irradiation time on the formation of nanobubbles

The effect of microwave power was also studied. All water samples with initial oxygen of 15.0 mg/L were treated for 30 s by microwave at different working power. The yield of nanobubbles and the associated temperature profile were shown in Figure 5. The nanobubble formation was well correlated to the resulting temperature. An apparent improvement of nanobubbles yield was found between 300 and 400 W, where the resulting temperature was 34 - 52 °C. The nanobubbles density increased from 0.8 to 15 numbers/μm^2 by improving working power from 200 to 600 W, suggesting that increasing work power improved the yield of nanobubbles.

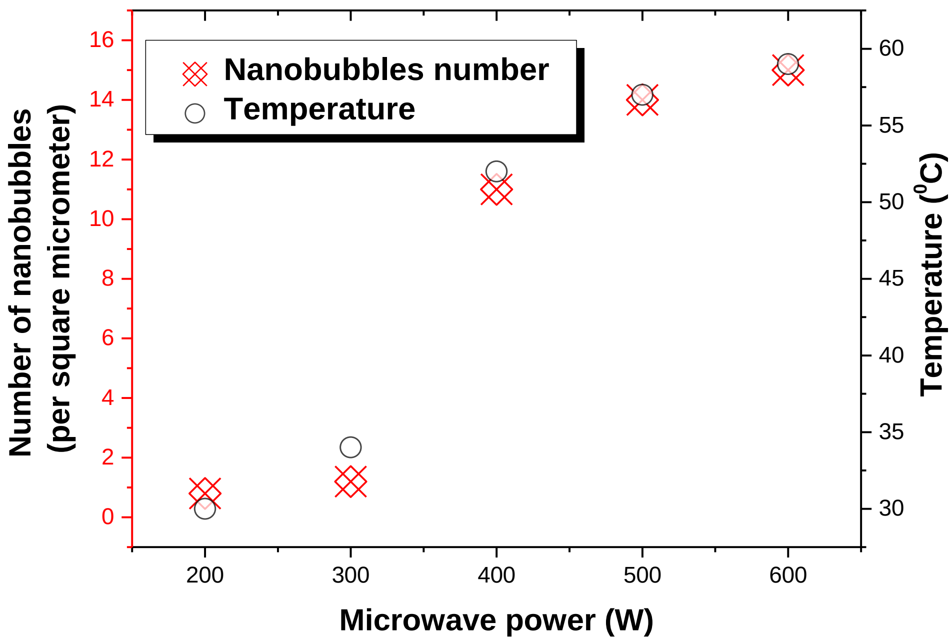

Figure 5. Effect of microwave power on the formation of nanobubbles

3.3. Oxygen concentration effect

Gas concentration was proved to be an important factor affecting the formation of nanobubbles.[56] In order to study the oxygen concentration effect, we prepared water with different initial oxygen concentrations from 11.3 to 30.0 mg/L. The initial temperature was 19 °C. Samples were treated 60 s by 300 W microwave irradiation and then followed with AFM measurement. The resulting temperature was 45 °C after switching off the microwave. Typical images of nanobubbles as function of oxygen concentration were shown in Figure 6. The yield of nanobubbles increased with increasing oxygen concentration (Figure 6e).

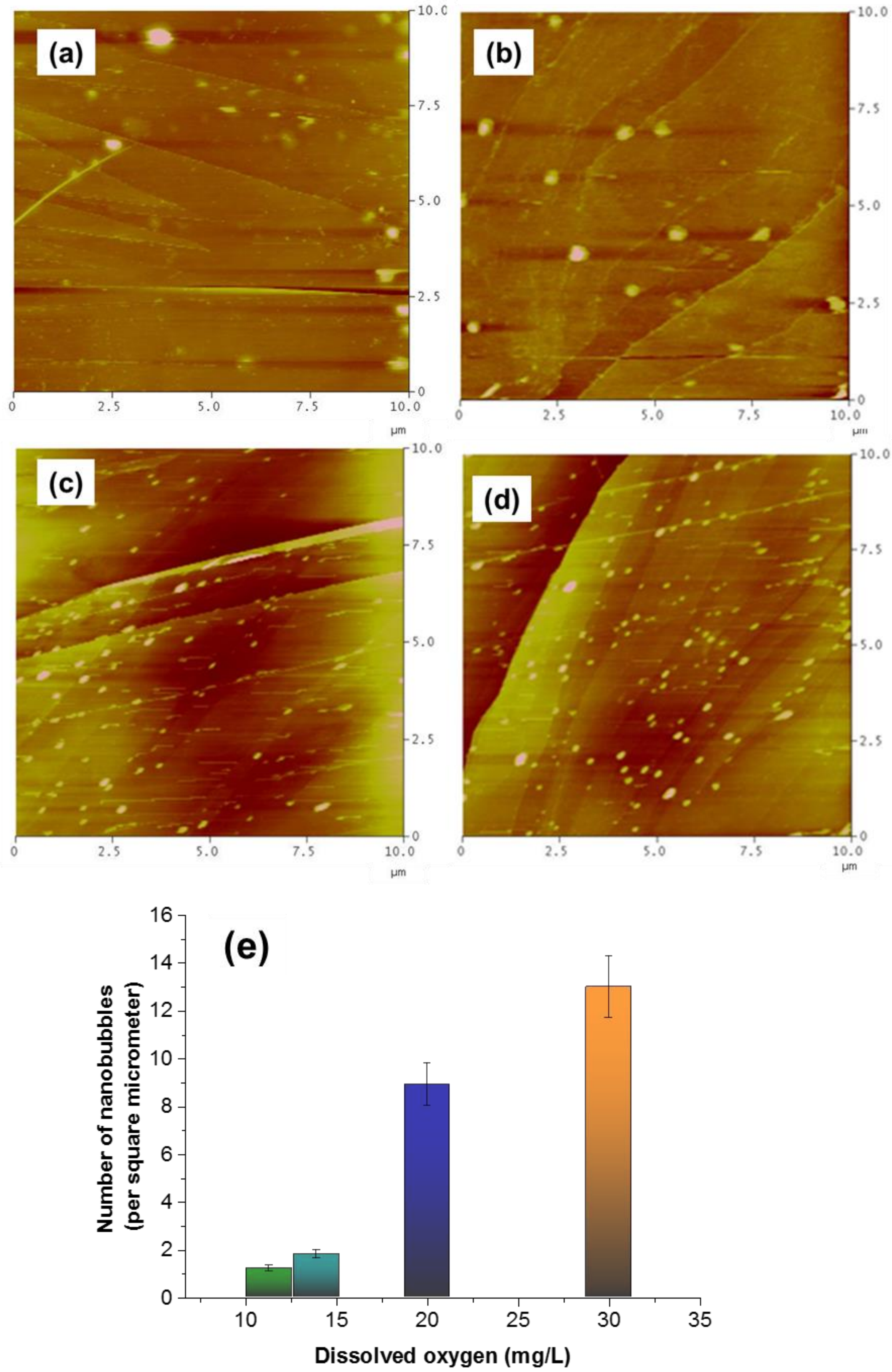

Figure 6. AFM height images of oxygen nanobubbles generated by microwave in water with different oxygen concentrations: (a) 11.3 mg/L,

(b) 13.9 mg/L, (c) 20.0 mg/L, (d) 30.0 mg/L and (e) the number of nanobubbles versus oxygen concentration. The scan sizes is 10 μm × 10 μm and height scale is 30 nm.

When HOPG was immerged in an oversaturated oxygen water with 30.0 mg/L of DO with no microwave treatment, no interfacial nanobubbles were observed (Figure 7).

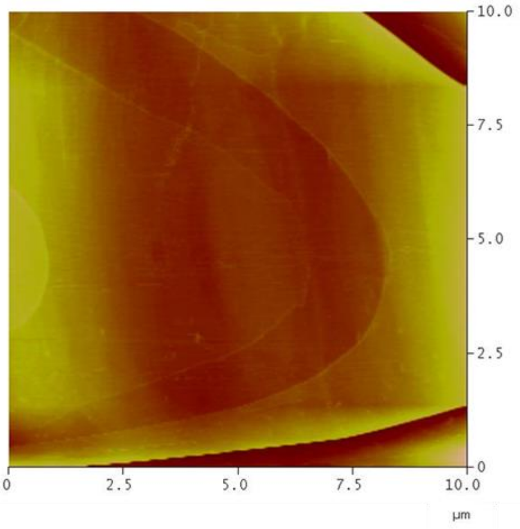

Figure 7. AFM image of HOPG surface in water with 30.0 mg/L of DO without microwave treatment

4. DISCUSSION

4.1. Generation of interfacial nanobubbles by microwave

It is well known that water molecule is polar with high dielectric constant (20 °C, 80 F/m) and dielectric loss factor, thus has strong ability to absorb microwave. Graphite displays strong microwave absorption ability and may yield "hot spots".[50, 51] Microwave treatment and temperature change in water are related (Table S1). The combination of hot HOPG substrate and temperature change in water by microwave irradiation may be responsible for the formation of interfacial nanobubbles. Experimental results demonstrated the yield of nanobubbles was well associated with the irradiation time and working power. The yield of nanobubbles increased about ten times when irradiation time increased from 60 s to 120 s by 200 W microwave treatment (Figure 4). The nanobubbles density increased from 0.8 to 15 numbers/μm^2 by improving work power from 200 to 600 W (Figure 5). Microwave irradiation significantly enhanced nanobubble generation. By adjusting microwave working power or irradiation time, it is possible to achieve desired nanobubbles (amount and size) quickly and conveniently.

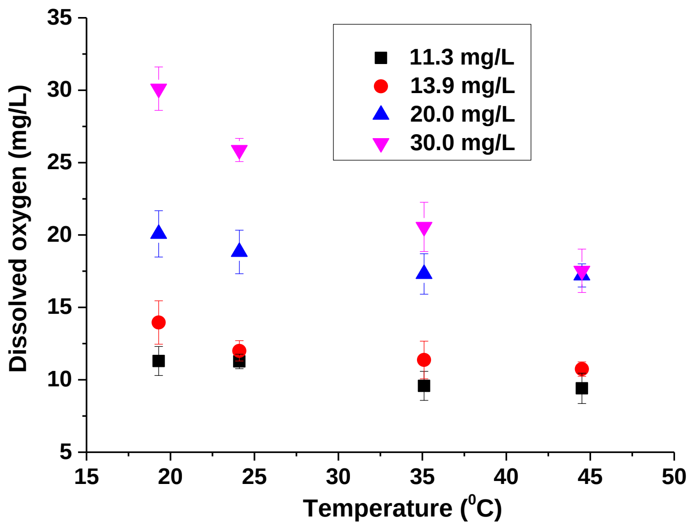

Figure 8. Oxygen concentration versus system temperature

Gas concentration played an important role on the nanobubble formation.[56, 57] Figure 8 shows the relationship between the oxygen concentration in water solution and the temperature variation caused by microwave irradiation. The higher initial concentration of oxygen, the more oxygen released from aqueous phase and thus induced the nanobubble nucleation. The yield of nanobubble was apparently increased from 1.2 to 13 numbers/μm^2 when initial oxygen was increased from 11.3 to 30 mg/L (Figure 6). While the yield of oxygen nanobubbles can be largely manipulated by oxygen concentration, it remains an interesting topic to study their stability under various water conditions such as the oxygen delivery effect in aerobic environment.

4.2. Possible mechanism of nanobubble formation

In this study, nanobubbles were not observed by AFM when the freshly cleaved HOPG substrate was immersed into water with rather high oxygen concentration (9.0 - 30 mg/L) at ambient environment without microwave treatment (Figure 2a and Figure 7). This agreed with literature that few nanobubbles can be detected simply by immersing a hydrophobic substrate into water.[20, 57, 58] Zhang et al.[59] reported that interfacial nanobubbles were not observed when a smooth OTS-Si wafer was put in a CO_2 saturated water solution, and the interfacial bubbles are only formed through a fast solvent exchange treatment. It is widely accepted that the fast variation of gas solubility in water solution is key in inducing the nucleation of nanobubbles.

In this work, oxygen solubility in water was rapidly decreased with the temperature increase caused by microwave treatment (Figure 8). The positive/negative direction of electric field in the microwave could change

2.45 billion times per second.[50] The fast changing electric fields of the microwave radiation lead to a rotation of the water molecule. The fast water shear flow and molecules friction can open the hydrogen bond between oxygen and water molecule and result in the decrease of oxygen solubility in the aqueous solution. This is a physical process caused by microwave non-thermal effect.[54] Meantime, severe temperature variation by microwave thermal effect also helped to decrease the oxygen solubility. The nanobubble formation mechanism is described in the schematic diagram of Figure 9. One possible pathway is that interfacial nanobubbles could be formed by direct oxygen molecule nucleation and accumulated on HOPG surface as nanoscale gas state. When irradiated by the microwaves, HOPG could absorb microwave energy and result in a rapid heating of the surface. The violent release of heat by the HOPG resulted in a rapid decrease of gas solubility in the surrounding domain, which contribute to the nanobubble nucleation on HOPG-water surface. Another possible pathway is that free oxygen nanobubbles could be formed in the bulk solution and then attached to HOPG surface to form surface nanobubbles.[16] Due to the strong microwave absorption ability, both water and HOPG substrate temperature could be well controlled by microwave, which is different from the non-selective temperature change method.[35] In addition, the selective heating by microwave may be more energy efficient than the conventional heating conduction through the whole media.

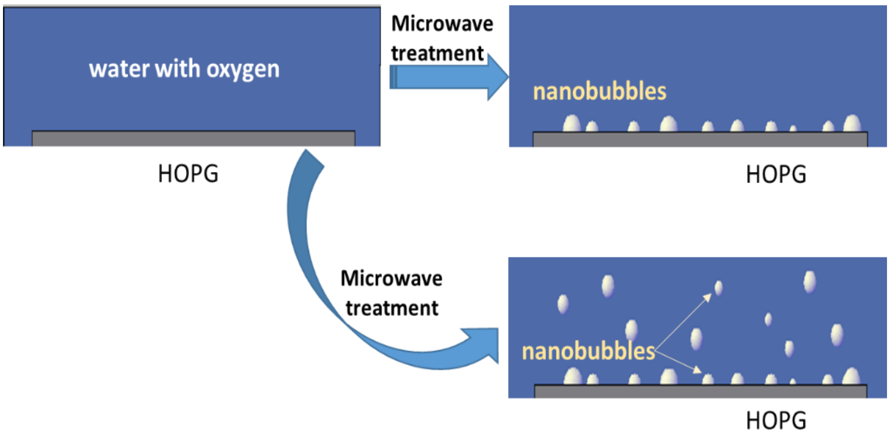

Figure 9. The possible mechanism of nanobubbles formation

4.3. Potential impacts

This work confirmed that microwave irradiation was an effective way in preparing surface nanobubbles. In order to present direct evidence of nanobubbles, oxygen nanobubbles was generated and determined on HOPG surface in this study. Recent study demonstrated that oxygen nanobubbles could be quantified at particle-water interfaces by scanning transmission soft X-ray microscopy.[60] The controlled formation of nanobubbles via microwave maybe valuable in preparing surface nanobubbles at various solid surfaces for practical applications, such as catalysis, hypoxia/anoxia remediation or as templates to prepare nanoscale materials. It is interesting to study whether other gas type of nanobubbles can be produced by microwave treatment. It remains a challenge in the future to study the many mysteries related to nanobubbles such as the gas density inside nanobubbles and the stability on particle surfaces.

5. CONCLUSIONS

This work found that surface nanobubbles can be generated by microwave treatment. The yield of nanobubbles can be manipulated by adjusting the irradiation and gas concentration. Both thermal and non-thermal effects of microwave may be responsible for the formation of nanobubble nucleation due to the decrease of oxygen solubility in aqueous system. The study provides a quick and convenient way to produce nanobubbles that may be useful for various applications.

ACKNOWLEDGMENTS

This work was supported by Strategic Priority Research Program of the Chinese Academy of Sciences (XDA09030203), National Natural Science Foundation of China (21407160) and the Science Promotion Program of Research Center for Eco-environmental Sciences, CAS (YSW2013B05).

REFERENCES

1. Parker, J. L.; Claesson, P. M.; Attard, P. Bubbles, cavities, and the long-ranged attraction between hydrophobic surfaces. *J. Phys. Chem.* **1994,** *98* (34), 8468-8480.
2. Ishida, N.; Inoue, T.; Miyahara, M.; Higashitani, K. Nano bubbles on a hydrophobic surface in water observed by tapping-mode atomic force microscopy. *Langmuir* **2000,** *16* (16), 6377-6380.
3. Lou, S. T.; Ouyang, Z. Q.; Zhang, Y.; Li, X. J.; Hu, J.; Li, M. Q.; Yang, F. J. Nanobubbles on solid surface imaged by atomic force microscopy. *J. Vac. Sci. Technol. B* **2000,** *18* (5), 2573-2575.
4. Wang, Y.; Bhushan, B. Boundary slip and nanobubble study in micro/nanofluidics using atomic force microscopy. *Soft matter* **2010,** *6* (1), 29-66.
5. Cavalli, R.; Bisazza, A.; Giustetto, P.; Civra, A.; Lembo, D.; Trotta, G.; Guiot, C.; Trotta, M. Preparation and characterization of dextran nanobubbles for oxygen delivery. *Int. J. Pharmaceut.* **2009,** *381* (2), 160-165.
6. Chang, S.; Si, T.; Zhang, S.; Merrick, M. A.; Cohn, D. E.; Xu, R. X. Ultrasound mediated destruction of multifunctional microbubbles for image guided delivery of oxygen and drugs. *Ultrason. Sonochem.* **2016,** *28*, 31-38.
7. Belova, V.; Gorin, D. A.; Shchukin, D. G.; Moehwald, H. Controlled effect of ultrasonic cavitation on hydrophobic/hydrophilic surfaces. *Acs Appl. Mater. Inter.* **2011,** *3* (2), 417-425.
8. Ibrahimkutty, S.; Kim, J.; Cammarata, M.; Ewald, F.; Choi, J.; Ihee, H.; Plech, A. Ultrafast structural

dynamics of the photocleavage of protein hybrid nanoparticles. *Acs Nano* **2011,** *5* (5), 3788-3794.

9. Brooks, M. Impossibubbles. *New Sci.* **2012,** *215* (2872), 38-41.

10. Pan, G.; Yang, B.; Wang, D.; Chen, H.; Tian, B.; Zhang, M.; Yuan, X.; Chen, J. In-lake algal bloom removal and submerged vegetation restoration using modified local soils. *Ecol. Eng.* **2011,** *37* (2), 302-308.

11. Pan, G.; Dai, L.; Li, L.; He, L.; Li, H.; Bi, L.; Gulati, R. D. Reducing the recruitment of sedimented algae and nutrient release into the overlying water using modified soil/sand flocculation-capping in eutrophic lakes. *Environ. Sci. Technol.* **2012,** *46* (9), 5077-5084.

12. Li, H.; Pan, G. Simultaneous removal of harmful algal blooms and microcystins using microorganism- and chitosan-modified local soil. *Environ. Sci. Technol.* **2015,** *49* (10), 6249-6256.

13. Craig, V. S. J. Very small bubbles at surfaces-the nanobubble puzzle. *Soft matter* **2011,** *7* (1), 40-48.

14. Seddon, J. R. T.; Kooij, E. S.; Poelsema, B.; Zandvliet, H. J. W.; Lohse, D. Surface bubble nucleation stability. *Phys. Rev. Lett.* **2011,** *106* (5), 056101.

15. Dammer, S. M.; Lohse, D. Gas enrichment at liquid-wall interfaces. *Phys. Rev. Lett.* **2006,** *96* (20), 206101.

16. Pan, G.; Yang, B. Effect of surface hydrophobicity on the formation and stability of oxygen nanobubbles. *ChemPhyschem* **2012,** *13* (8), 2205-2212.

17. An, H.; Liu, G.; Atkin, R.; Craig, V. S. J. Surface nanobubbles in nonaqueous media: looking for nanobubbles in DMSO, formamide, propylene carbonate, ethylammonium nitrate, and propylammonium nitrate. *Acs Nano* **2015,** *9* (7), 7596-7607.

18. Peng, H.; Hampton, M. A.; Nguyen, A. V. Nanobubbles do not sit alone at the solid-iquid interface. *Langmuir* **2013,** *29* (20), 6123-6130.

19. Peng, H.; Birkett, G. R.; Nguyen, A. V. Origin of interfacial nanoscopic gaseous domains and formation of dense gas layer at hydrophobic solid-water interface. *Langmuir* **2013,** *29* (49), 15266-15274.

20. Zhang, X. H.; Maeda, N.; Craig, V. S. J. Physical properties of nanobubbles on hydrophobic surfaces in water and aqueous solutions. *Langmuir* **2006,** *22* (11), 5025-5035.

21. Yang, S.; Dammer, S. M.; Bremond, N.; Zandvliet, H. J. W.; Kooij, E. S.; Lohse, D. Characterization of nanobubbles on hydrophobic surfaces in water. *Langmuir* **2007,** *23* (13), 7072-7077.

22. Weijs, J. H.; Lohse, D. Why surface nanobubbles live for hours. *Phys. Rev. Lett.* **2013,** *110* (5), 054501.

23. Lohse, D.; Zhang, X. Pinning and gas oversaturation imply stable single surface nanobubbles. *Phys. Rev. E* **2015,** *91* (3), 031003.

24. Borkent, B. M.; Dammer, S. M.; Schoenherr, H.; Vancso, G. J.; Lohse, D. Superstability of surface nanobubbles. *Phys. Rev. Lett.* **2007,** *98* (20), 204502.

25. Lauga, E.; Brenner, M. P. Dynamic mechanisms for apparent slip on hydrophobic surfaces. *Phys. Rev. E* **2004,** *70* (2), 026311.

26. Liu, G.; Craig, V. S. J. Improved cleaning of hydrophilic protein-coated surfaces using the combination of nanobubbles and SDS. *Acs Appl. Mater. Inter.* **2009,** *1* (2), 481-487.

27. Liu, G.; Wu, Z.; Craig, V. S. J. Cleaning of protein-coated surfaces using nanobubbles: an investigation using a quartz crystal microbalance. *J. Phys. Chem. C* **2008,** *112* (43), 16748-16753.

28. Yang, S.; Duisterwinkel, A. Removal of nanoparticles from plain and patterned surfaces using nanobubbles. *Langmuir* **2011,** *27* (18), 11430-11435.

29. Calgaroto, S.; Wilberg, K. Q.; Rubio, J. On the nanobubbles interfacial properties and future applications in flotation. *Miner. Eng.* **2014,** *60*, 33-40.

30. Plowman, B. J.; Jones, L. A.; Bhargava, S. K. Building with bubbles: the formation of high surface area honeycomb-like films via hydrogen bubble templated electrodeposition. *Chem. Commun.* **2015,** *51* (21), 4331-4346.
31. Yang, J. W.; Duan, J. M.; Fornasiero, D.; Ralston, J. Very small bubble formation at the solid-water interface. *J. Phys. Chem. B* **2003,** *107* (25), 6139-6147.
32. Guo, W.; Shan, H.; Guan, M.; Gao, L.; Liu, M.; Dong, Y. Investigation on nanobubbles on graphite substrate produced by the water-NaCl solution replacement. *Surface Science* **2012,** *606* (17-18), 1462-1466.
33. Liu, M.; Zhao, W.; Wang, S.; Guo, W.; Tang, Y.; Dong, Y. Study on nanobubble generation: saline solution/water exchange method. *ChemPhyschem* **2013,** *14* (11), 2589-2593.
34. van Limbeek, M. A. J.; Seddon, J. R. T. Surface nanobubbles as a function of gas type. *Langmuir* **2011,** *27* (14), 8694-8699.
35. Lombard, J.; Biben, T.; Merabia, S. Nanobubbles around plasmonic nanoparticles: Thermodynamic analysis. *Phys. Rev. E* **2015,** *91* (4), 043007.
36. Zhang, L.; Zhang, Y.; Zhang, X.; Li, Z.; Shen, G.; Ye, M.; Fan, C.; Fang, H.; Hu, J. Electrochemically controlled formation and growth of hydrogen nanobubbles. *Langmuir* **2006,** *22* (19), 8109-8113.
37. Yang, S.; Tsai, P.; Kooij, E. S.; Prosperetti, A.; Zandvliet, H. J. W.; Lohse, D. Electrolytically generated nanobubbles on highly orientated pyrolytic graphite surfaces. *Langmuir* **2009,** *25* (3), 1466-1474.
38. Kikuchi, K.; Nagata, S.; Tanaka, Y.; Salhara, Y.; Ogumi, Z. Characteristics of hydrogen nanobubbles in solutions obtained with water electrolysis. *J. Electroanal. Chem.* **2007,** *600* (2), 303-310.
39. Kikuchi, K.; Tanaka, Y.; Saihara, Y.; Maeda, M.; Kawamura, M.; Ogumi, Z. Concentration of hydrogen nanobubbles in electrolyzed water. *J. Colloid Interf. Sci.* **2006,** *298* (2), 914-919.
40. Kikuchi, K.; Tanaka, Y.; Saihara, Y.; Ogumi, Z. Study of hydrogen nanobubbles in solution in the vicinity of a platinum wire electrode using double-potential step chronoamperometry. *Electrochim. Acta* **2006,** *52* (3), 904-913.
41. Zhang, X. H.; Li, G.; Maeda, N.; Hu, J. Removal of induced nanobubbles from water/graphite interfaces by partial degassing. *Langmuir* **2006,** *22* (22), 9238-9243.
42. Hampton, M. A.; Donose, B. C.; Nguyen, A. V. Effect of alcohol-water exchange and surface scanning on nanobubbles and the attraction between hydrophobic surfaces. *J. Colloid Interf. Sci.* **2008,** *325* (1), 267-274.
43. Lachaine, R.; Boulais, E.; Meunier, M. From thermo- to plasma-mediated ultrafast laser-induced plasmonic nanobubbles. *Acs Photonics* **2014,** *1* (4), 331-336.
44. Baffou, G.; Polleux, J.; Rigneault, H.; Monneret, S. Super-heating and micro-bubble generation around plasmonic nanoparticles under cw illumination. *J. Phys. Chem. C* **2014,** *118* (9), 4890-4898.
45. Boulais, E.; Lachaine, R.; Hatef, A.; Meunier, M. Plasmonics for pulsed-laser cell nanosurgery: Fundamentals and applications. *J. Photoch. Photobio. C* **2013,** *17*, 26-49.
46. Kitz, M.; Preisser, S.; Wetterwald, A.; Jaeger, M.; Thalmann, G. N.; Frenz, M. Vapor bubble generation around gold nanoparticles and its application to damaging of cells. *Biomed. Opt. Express* **2011,** *2* (2), 291-304.
47. Chen, Q.; Luo, L.; White, H. S. Electrochemical generation of a hydrogen bubble at a recessed platinum nanopore electrode. *Langmuir* **2015,** *31* (15), 4573-4581.
48. Kikuchi, K.; Ioka, A.; Oku, T.; Tanaka, Y.; Saihara, Y.; Ogumi, Z. Concentration determination of oxygen nanobubbles in electrolyzed water. *J. Colloid Interf. Sci.* **2009,** *329* (2), 306-309.
49. Chen, Q.; Wiedenroth, H. S.; German, S. R.; White, H. S. Electrochemical nucleation of stable N_2

nanobubbles at Pt nanoelectrodes. *J. Am. Chem. Soc.* **2015,** *137* (37), 12064-12069.
50. Nuchter, M.; Ondruschka, B.; Bonrath, W.; Gum, A. Microwave assisted synthesis - a critical technology overview. *Green Chem.* **2004,** *6* (3), 128-141.
51. Nie, H.; Zhang, T.; Cui, M.; Lu, H.; Lovley, D. R.; Russell, T. P. Improved cathode for high efficient microbial-catalyzed reduction in microbial electrosynthesis cells. *Phys. Chem. Chem. Phys.* **2013,** *15* (34), 14290-14294.
52. Zheng, J.; Liu, H.; Wu, B.; Guo, Y.; Wu, T.; Yu, G.; Liu, Y.; Zhu, D. Production of high-quality carbon nanoscrolls with microwave spark assistance in liquid nitrogen. *Adv. Mater.* **2011,** *23* (21), 2460-2463.
53. Luo, Z.; Lu, Y.; Somers, L. A.; Johnson, A. T. C. High yield preparation of macroscopic graphene oxide membranes. *J. Am. Chem. Soc.* **2009,** *131* (3), 898-899.
54. Wroe, R.; Rowley, A. T. Evidence for a non-thermal microwave effect in the sintering of partially stabilized zirconia. *J. Mater. Sci.* **1996,** *31* (8), 2019-2026.
55. Xu, C.; Peng, S.; Qiao, G. G.; Gutowski, V.; Lohse, D.; Zhang, X. Nanobubble formation on a warmer substrate. *Soft matter* **2014,** *10* (39), 7857-7864.
56. German, S. R.; Wu, X.; An, H.; Craig, V. S. J.; Mega, T. L.; Zhang, X. Interfacial nanobubbles are leaky: permeability of the gas/water interface. *Acs Nano* **2014,** *8* (6), 6193-6201.
57. McKee, C. T.; Ducker, W. A. Refractive index of thin, aqueous films between hydrophobic surfaces studied using evanescent wave atomic force microscopy. *Langmuir* **2005,** *21* (26), 12153-12159.
58. Takata, Y.; Cho, J. H. J.; Law, B. M.; Aratono, M. Ellipsometric search for vapor layers at liquid-hydrophobic solid surfaces. *Langmuir* **2006,** *22* (4), 1715-1721.
59. Zhang, X. H.; Quinn, A.; Ducker, W. A. Nanobubbles at the interface between water and a hydrophobic solid. *Langmuir* **2008,** *24* (9), 4756-4764.
60. Pan, G.; He, G.; Zhang, M.; Zhou, Q.; Tyliszczak, T.; Tai, R.; Guo, J.; Bi, L.; Wang, L.; Zhang, H. Nanobubbles at hydrophilic particle water interfaces. *Langmuir* **2016,** *DOI: 10.1021/acs.langmuir.6b01483*.

Table of Contents